Ann Surg Oncol (2014) 21:3564–3571
DOI 10.1245/s10434-014-3760-0

Annals of
SURGICAL ONCOLOGY
OFFICIAL JOURNAL OF THE SOCIETY OF SURGICAL ONCOLOGY

ORIGINAL ARTICLE – BONE AND SOFT TISSUE SARCOMAS

Nomogram Predicting Severe Adverse Events After Musculoskeletal Tumor Surgery: Analysis of a National Administrative Database

Koichi Ogura, MD[1], Hideo Yasunaga, MD, PhD[2], Hiromasa Horiguchi, PhD[3], Kiyohide Fushimi, MD, PhD[4], Sakae Tanaka, MD, PhD[1], and Hirotaka Kawano, MD, PhD[1]

[1]Department of Orthopaedic Surgery, The University of Tokyo Hospital, Tokyo, Japan; [2]Department of Health Economics and Epidemiology Research, School of Public Health, The University of Tokyo, Tokyo, Japan; [3]Department of Clinical Data Management and Research, Clinical Research Center, National Hospital Organization Headquarters, Tokyo, Japan; [4]Department of Health Policy and Informatics, Tokyo Medical and Dental University Graduate School of Medicine, Tokyo, Japan

ABSTRACT

Background. There have been no nationwide surveys of postoperative adverse events (AEs) after musculoskeletal tumor surgery focusing on their severity. Therefore, we developed a nomogram to predict severe AEs after musculoskeletal tumor surgery.

Methods. We identified patients in the Diagnosis Procedure Combination database who underwent musculoskeletal tumor surgery during 2007–2012, and defined severe AEs as follows: (i) in-hospital mortality; (ii) postoperative medications including massive transfusion (≥1,400 mL), catecholamines, γ-globulin products, protease inhibitors, and medications for disseminated intravascular coagulation; and (iii) postoperative interventions consisting of mechanical ventilation, dialysis support, and cardiac support. Logistic regression models were used to address the occurrence of severe AEs.

Results. Of 5,716 patients identified, 613 patients (10.7 %) had severe AEs. Multivariate analyses showed an inverse relationship between body mass index (BMI) and severe AEs (odds ratio 1.80 for BMI <18.50; $p < 0.001$) after adjustment for other significant factors, including sex, age, tumor location, Charlson comorbidity index, type of surgery, and duration of anesthesia. A nomogram and a calibration plot based on these results were well-fitted to predict the probability of severe AEs after musculoskeletal tumor surgery (concordance index 0.781).

Conclusions. We developed a nomogram predicting the probability of severe AEs after musculoskeletal tumor surgery. In addition, we clarified that underweight, but not overweight or obese, status was significantly associated with increased severe AEs after adjusting for patient background characteristics.

It is widely recognized that patients undergoing musculoskeletal tumor surgery are at increased risk of postoperative adverse events (AEs) compared with those undergoing general orthopedic surgery, owing to the more invasive nature of the surgical procedures, and the generally poorer condition of patients with tumors who have undergone preoperative chemotherapy. To date, postoperative AEs in musculoskeletal tumor surgery, such as surgical site infection or venous thromboembolism, have been reported based on limited data from single centers or a few major referral centers.[1–6] However, these reports did not focus on the severity of the AEs.

Given the above-mentioned nature of musculoskeletal tumor surgery, and despite the development of perioperative management, we hypothesized that musculoskeletal tumor surgery would be associated with higher rates of postoperative severe AEs demanding postoperative medications or interventions. However, to our knowledge, there have been no nationwide surveys of severe AEs after musculoskeletal tumor surgery, and the factors affecting the incidence of severe AEs in musculoskeletal tumor surgery remain unclear.

First Received: 25 February 2014;
Published Online: 7 May 2014

H. Kawano, MD, PhD
e-mail: hkawano-tky@umin.net

Therefore, we investigated the nationwide incidence of severe AEs after musculoskeletal tumor surgery in Japan and analyzed the risk factors associated with the incidence of severe AEs by analyzing data from the Diagnosis Procedure Combination (DPC) database, which is a nationally representative inpatient database in Japan. In addition, we developed a nomogram to predict the occurrence of severe AEs after musculoskeletal tumor surgery.

PATIENTS AND METHODS

Data Source

The DPC database is a national administrative claims and discharge abstract database for acute-care inpatients in Japan, the details of which were described elsewhere.[7–10] Data were collected over 6 months (from 1 July to 31 December) until 2010, and throughout the year from 2011. The numbers of cases in the database were 2.7, 2.8, 2.8, 3.3, and 7.0 million in 2007, 2008, 2009, 2010, and 2011, respectively, representing approximately 50 % of all inpatient admissions to secondary and tertiary care hospitals in Japan. There are 89 Japanese orthopaedic association (JOA)-certified hospitals that specialize in the treatment of musculoskeletal tumors in Japan. Eighty-seven of these hospitals (66 academic hospitals and 21 non-academic hospitals) are included in the DPC database. A total of 4,685 patients (82.0 %) who underwent surgery for musculoskeletal tumors were treated in academic hospitals (JOA-certified or non-JOA-certified; 3,386 patients, 59.3 %) or JOA-certified non-academic hospitals (cancer treatment centers; 1,299 patients, 22.7 %).

The database includes the following data for each patient: location of hospital; age; sex; diagnoses and comorbidities at admission and complications after admission recorded with text data in the Japanese language and the International classification of diseases, 10th revision (ICD-10) codes; procedures coded with Japanese original codes; drugs and devices used; length of stay; and discharge status. Complications that occurred after admission are clearly differentiated from comorbidities that were already present at admission.

Owing to the anonymous nature of the data, informed consent was waived. Study approval was obtained from the Institutional Review Board of The University of Tokyo.

Data Extraction

We identified the records of all patients in the DPC database who underwent musculoskeletal tumor surgery during 2007–2012. For each patient, we extracted the following data: patient characteristics (sex, age, body mass index [BMI], comorbidities); details of disease (main diagnosis, tumor location); details of surgery (type of surgery, volume of perioperative blood transfusion, duration of anesthesia); and postoperative length of stay. We extracted comorbidities that may affect the rates of severe AEs, including diabetes mellitus (ICD-10 codes E10.x–E14.x), chronic lung disease (I27.8, I27.9, J40.x–J47.x, J60.x–J67.x, J68.4, J70.1, J70.3), cardiac disease (I25.2, I09.9, I11.0, I13.0, I13.2, I20.x, I21.x, I22.x, I25.5, I42.0, I42.5–I42.9, I43.x, I50.x, P29.0), cerebrovascular disease (G45.x, G46.x, H34.0, I60.x–I69.x), chronic renal failure (N18.x), and liver disease (I85.0, I85.9, I86.4, I98.2, K70.4, K71.1, K72.1, K72.9, K76.5, K76.6, K76.7). Based on Quan's protocol, each ICD-10 code of a comorbidity was converted into a score, and the sum of the scores was used to calculate the patient's Charlson comorbidity index (CCI).[11]

BMI was computed using the following standard equation: BMI = weight in kg/height squared in meters. BMI was categorized into five groups: <18.50 (underweight); 18.50–22.99 (lower normal range); 23.00–24.99 (upper normal range); 25.00–29.99 (overweight); and ≥30.00 (obese).[12] Diagnoses were categorized into two groups: primary malignant bone tumor (ICD-10 codes C40.x, C41.x), and primary malignant soft tissue tumor (C47.x, C48.0, C49.x). The tumor locations were categorized into three subgroups: upper extremity, lower extremity, and trunk. The types of surgery were also categorized into three subgroups: bone tumor resection (Japanese original procedure code K053), soft tissue tumor resection (K031), and amputation (K084). Although the DPC database does not include information on the operation time, it is generally reflected by the anesthesia time. The durations of anesthesia were categorized into three subgroups: <120 min, 120–240 min, and >240 min. The hospital volumes for all musculoskeletal surgery were determined using the unique identifier for each hospital. Patients were divided into tertiles according to hospital volume (number of musculoskeletal surgery cases per year) so that the number of patients in each group was almost equal. As a result, low volume was defined as ≤13 cases/year, medium volume as 14–28 cases/year, and high volume as ≥29 cases/year.

Endpoints

We defined a severe AE as a status involving at least one of the following conditions: (i) in-hospital morality; (ii) postoperative medications, including massive blood transfusion (≥1,400 mL), catecholamines (strong vasopressors: dopamine, dobutamine, adrenaline, noradrenaline), protease inhibitors (used for shock status: gabexate mesilate, nafamostat mesilate, ulinastatin), γ-globulin products (used for severe septic shock), and anti-disseminated intravascular coagulation (DIC) medications (dalteparin sodium,

TABLE 1 Characteristics of the study population according to surgical procedures

	Overall ($N = 5,716$)	Soft tissue tumor resection ($N = 4,534$)	Bone tumor resection ($N = 896$)	Amputation ($N = 286$)	p value
Age, years (mean (SD))	58.0 (20.2)	60.5 (18.4)	45.9 (23.0)	55.7 (23.5)	<0.001
≤64	3,183 (55.7)	2,373 (52.3)	643 (71.8)	167 (58.4)	
65–79	1,845 (32.3)	1,551 (34.2)	218 (24.3)	76 (26.6)	
≥80	688 (12.0)	610 (13.5)	35 (3.9)	43 (15.0)	
Sex					
Male	3,129 (54.7)	2,463 (54.3)	496 (55.4)	170 (59.4)	0.222
Female	2,587 (45.3)	2,071 (45.7)	400 (44.6)	116(40.6)	
Tumor site					
Upper extremity	846 (14.8)	719(15.9)	65 (7.3)	62 (21.7)	<0.001
Lower extremity	2,698 (47.2)	2,261 (49.9)	292 (32.6)	145 (50.7)	
Trunk	1,718 (30.1)	1,144 (25.2)	519(57.9)	55 (19.2)	
Data not provided	454 (7.9)	410 (9.0)	20 (2.2)	24 (8.4)	
CCI					
2	4,206 (73.6)	3,345 (73.8)	676 (75.4)	185 (64.7)	<0.001
3	863 (15.1)	710 (15.7)	113 (12.6)	40 (14.0)	
≥4	647 (11.3)	149 (10.5)	107 (12.0)	61 (21.3)	
BMI					
<18.50	405 (7.1)	257(5.7)	113 (12.6)	35 (12.2)	<0.001
18.50–22.99	1,475 (25.8)	1,137(25.1)	256 (28.6)	82 (28.7)	
23.00–24.99	737 (12.9)	627(13.8)	81 (9.0)	29 (10.1)	
25.00–29.99	863 (15.1)	741 (16.3)	89 (9.9)	33 (11.5)	
≥30.0	136 (2.4)	115 (2.5)	18 (2.0)	3 (1.0)	
Data not provided	2,100 (36.7)	1,657(36.5)	339 (37.8)	104 (36.4)	
Blood transfusion, mL (median (IQR))	840 (560–1,620)	560 (400–1,120)	1,120 (560–1,960)	840 (560–1,680)	<0.001
No	4,702 (82.3)	4,058 (89.5)	438 (48.9)	206 (72.0)	<0.001
Yes	1,014 (17.7)	476 (10.5)	458 (51.1)	80 (28.0)	
Anesthesia time, min (median (IQR))	216 (142–345)	195 (135–307)	379 (251–567)	204 (157–278)	<0.001
≤120	932 (16.6)	862 (19.3)	44 (5.1)	26 (9.2)	<0.001
121–240	2,261 (40.3)	1,851 (43.8)	159(18.3)	151 (53.5)	
>240	2,417(43.1)	1,646 (36.9)	666 (76.6)	105 (37.2)	
Postoperative length of stay, days (median (IQR))	19 (11–35)	17 (11–29)	35 (19–66)	29 (17–56)	<0.001

SD standard deviation, *CCI* Charlson comorbidity index, *BMI* body mass index, *IQR* interquartile range

danaparoid sodium, human anti-thrombin III, thrombomodulin a); and (iii) postoperative interventions consisting of mechanical ventilation (Japanese procedure codes J044.1, J045.x), dialysis support (J038.x–J039, J041.x–J042), and cardiac support, including chest compression (J046), use of defibrillator (J047), open cardiac massage (K545), intra-aortic balloon pumping (K600), and use of extracorporeal circulation devices such as percutaneous cardiopulmonary support (K602) and ventricular assisting devices (K603). We were able to differentiate between preoperative and perioperative treatments because the DPC administrative data included information on the dates when each drug, device, or procedure was used for the individual patients.

Statistical Analyses

A univariate logistic regression analysis was performed with each covariate for the prediction of severe AEs. We then constructed a multivariate logistic regression model excluding insignificant factors at a significance level of <10 % in the univariate model. Based on the results, we built a nomogram to predict the occurrence of severe AEs. Internal validation was performed via a bootstrap method with 50 resamples, and a calibration plot was derived to evaluate the relationship between predicted probabilities by the nomogram and observed rates. In univariate comparisons, categorical variables were compared by the Chi square test, and continuous variables were compared by the

TABLE 2 Distribution of severe adverse events for each surgical procedure

	Overall ($N = 5,716$)	Soft tissue tumor resection ($N = 4,534$)	Bone tumor resection ($N = 896$)	Amputation ($N = 286$)	p value
Overall (N (^{0} %))	613 (10.7)	312 (6.9)	244 (27.2)	57 (19.9)	<0.001
Postoperative medications (N (%))					
Massive transfusion	313 (5.5)	102 (2.2)	184 (20.5)	27 (9.4)	<0.001
Catecholamines	290 (5.1)	174 (3.8)	90 (10.0)	26 (9.1)	<0.001
Protease inhibitors	72 (1.3)	43 (0.9)	22 (2.5)	7 (2.4)	<0.001
γ-globulin products	53 (0.9)	24 (0.5)	25 (2.8)	4(1.4)	<0.001
Anti-DIC medications	28 (0.5)	13 (0.3)	13 (1.5)	2 (0.7)	<0.001
Postoperative intervention (N (%))					
Mechanical ventilation	60 (1.0)	25 (0.6)	32 (3.6)	3 (1.0)	<0.001
Dialysis support	36 (0.6)	24 (0.5)	8 (0.9)	4 (1.4)	0.110
Cardiac support	11 (0.2)	5 (0.1)	4 (0.4)	2 (0.7)	0.015
In-hospital death (N (%))	45 (0.8)	30 (0.7)	9(1.0)	6 (2.1)	0.021

DIC disseminated intravascular coagulation

Mann–Whitney U test. The threshold for significance was a value of $p < 0.05$. All statistical analyses were conducted using IBM SPSS version 19.0 (IBM Corporation, Armonk, NY, USA) and the nomogram was built by R version 3.0.1 (R Foundation for Statistical Computing, Vienna, Austria) with the rms library.

RESULTS

During a total period of 39 months (1 July to 31 December of 2007–2010; 1 January to 31 December of 2011; and 1 January to 31 March of 2012), data for about 20 million inpatients were collected in the DPC database. We identified 5,716 eligible patients who underwent surgery, including bone tumor resection (Japanese procedure code K053), soft tissue tumor resection (K031), and amputation (K084) for primary malignant bone tumors (ICD-10 codes C40.x, C41.x) or primary malignant soft tissue tumors (C47.x, C48.0, C49.x). The background characteristics of the patients and details of their surgery according to surgical procedures are shown in Table 1. The patients comprised 3,129 males and 2,587 females with a mean (±SD) age of 58.0 ± 20.2 years. The type of surgery was bone tumor resection in 896 patients, soft tissue tumor resection in 4,534 patients, and amputation in 286 patients.

In the CCI, 'malignant tumor' is assigned a score of 2. Therefore, approximately 26 % of patients were classified as having comorbidities. The duration of anesthesia was 120 min or longer in the majority of patients, with a median (interquartile range) duration of 216 (142–345) min. The duration of anesthesia was relatively long in the bone tumor resection group. The postoperative length of stay was also relatively long in the bone tumor resection group.

Table 2 shows the distribution of severe AEs in each surgical procedure. Overall, 613 patients (10.7 %) met the criteria for severe AEs, including 45 in-hospital deaths (0.8 %). Severe AEs were most frequent in the bone tumor resection group (244 patients; 27.2 %). Postoperative medications included massive transfusion in 313 patients (5.5 %), catecholamines in 290 patients (5.1 %), protease inhibitors in 72 patients (1.3 %), γ-globulin products in 53 patients (0.9 %), and anti-DIC medications in 28 patients (0.5 %). Postoperative interventions included mechanical ventilation in 60 patients (1.0 %), dialysis support in 36 patients (0.6 %), and cardiac support in 11 patients (0.2 %).

Table 3 shows univariate and multivariate logistic regression analyses for severe AEs. The univariate analyses showed that tumor location, CCI, BMI, type of surgery, and duration of anesthesia were significantly associated with severe AEs. The multivariate logistic regression analyses showed significant associations between severe AEs and age of 65–79 years (odds ratio [OR] 1.28; 95 % CI 1.04–1.58; $p = 0.018$) or ≥80 years (OR 1.81; 95 % CI 1.35–2.43; $p < 0.001$), tumor location of trunk (OR 1.54; 95 % CI 1.11–2.14; $p = 0.009$), CCI of 3 (OR 1.33; 95 % CI 1.03–1.71; $p = 0.027$) or ≥4 (OR 1.94; 95 % CI 1.52–2.48; $p < 0.001$), BMI of <18.50 (OR 1.80; 95 % CI 1.30–2.50; $p < 0.001$), type of surgery involving bone tumor resection (OR 3.23; 95 % CI 2.60–4.02; $p < 0.001$) or amputation (OR 3.46; 95 % CI 2.48–4.84; $p < 0.001$), and duration of anesthesia of >240 min (OR 5.41; 95 % CI 3.62 to −8.08; $p < 0.001$).

TABLE 3 Univariate and multivariate logistic regression analyses for severe adverse events

	No. of patients (%)	No. of patients with severe AEs (%)	Univariate analysis		Multivariate analysis	
			Odds ratio (95 % CI)	p value	Odds ratio (95 % CI)	*p* value
Total no. of patients	5,716	613 (10.7)				
Sex						
Male	3,129 (54.7)	348 (11.1)	Reference		Reference	
Female	2,587 (45.3)	265 (10.2)	0.91 (0.77–1.08)	0.286	0.98 (0.82–1.18)	0.848
Age, years						
≤64	3,183 (55.7)	343 (10.8)	Reference		Reference	
65–79	1,845 (32.3)	193 (10.5)	0.97 (0.80–1.17)	0.727	1.28 (1.04–1.75)	0.017
≥80	688 (12.0)	77 (11.2)	1.04 (0.80–1.36)	0.750	1.81 (1.35–2.43)	<0.001
Tumor location						
Upper extremity	846 (14.8)	57 (6.7)	Reference		Reference	
Lower extremity	2,698 (47.2)	257 (9.5)	1.46 (1.08–1.96)	0.013	1.28 (0.93–1.75)	0.129
Trunk	1,718 (30.1)	257 (15.0)	2.44 (1.80–3.29)	<0.001	1.54 (1.11–2.13)	0.010
Data not provided	454 (7.9)	42 (9.3)	1.411 (0.931–2.139)	0.105	1.50 (0.97–2.34)	0.070
CCI						
2	4,206 (73.6)	388 (9.2)	Reference		Reference	
3	863 (15.1)	102 (11.8)	1.32 (1.05–1.66)	0.019	1.34 (1.04–1.72)	0.023
≥4	647 (11.3)	123 (19.0)	2.31 (1.85–2.89)	<0.001	1.94 (1.52–2.48)	<0.001
BMI						
<18.50	405 (7.1)	82 (20.2)	2.06 (1.54–2.76)	<0.001	1.80 (1.30–2.50)	<0.001
18.50–22.99	1,475 (25.8)	162 (11.0)	Reference		Reference	
23.00–24.99	737 (12.9)	75 (10.2)	0.92 (0.69–1.23)	0.563	1.00 (0.73–1.37)	0.994
25.00–29.99	863 (15.1)	75 (8.7)	0.77 (0.58–1.03)	0.077	0.88 (0.64–1.19)	0.404
≥30.0	136 (2.4)	14 (10.3)	0.93 (0.52–1.66)	0.805	1.13 (0.61–2.07)	0.705
Data not provided	2,100 (36.7)	205 (9.8)	0.88 (0.71–1.09)	0.237	0.92 (0.73–1.17)	0.504
Type of surgery						
Soft tissue tumor resection	4,534 (79.3)	312 (6.9)	Reference		Reference	
Bone tumor resection	896 (15.7)	244 (27.2)	5.06 (4.20–6.10)	<0.001	3.24 (2.61–4.03)	<0.001
Amputation	286 (5.0)	57 (19.9)	3.37 (2.47–4.60)	<0.001	3.50 (2.50–4.90)	<0.001
Duration of anesthesia (min)						
<120	932 (16.6)	28 (3.0)	Reference		Reference	
120–240	2,261 (40.3)	102 (4.5)	1.53 (0.99–2.33)	0.052	1.36 (0.88–2.09)	0.166
>240	2,417 (43.1)	469 (19.4)	7.77 (5.27–11.47)	<0.001	5.69 (3.82–8.49)	<0.001

AEs adverse events, *CI* confidence interval, *CCI* Charlson comorbidity index, *BMI* body mass index

Based on these results, we developed a nomogram that visually showed the multivariate impact of each variable (Fig. 1). The concordance index of the model was 0.781. The calibration plots are shown in Fig. 2. The differences between the observed rates and predicted probabilities were within 0.015 for 90 % of patients.

DISCUSSION

In the present study, we analyzed 5,716 patients who underwent primary musculoskeletal tumor surgery between 2007 and 2012 using a nationwide inpatient database with a special emphasis on the severity of AEs, by defining a severe AE as a status requiring postoperative medications or interventions that reflected actual life-threatening conditions. Although there have been no previous reports describing the severity of these postoperative AEs, we revealed the significant risk factors for severe AEs after adjustment for patient background characteristics.

The overall incidence of severe AEs was 10.7 %, including 45 deaths (0.8 %). In the present study, we clarified the significant risk factors associated with

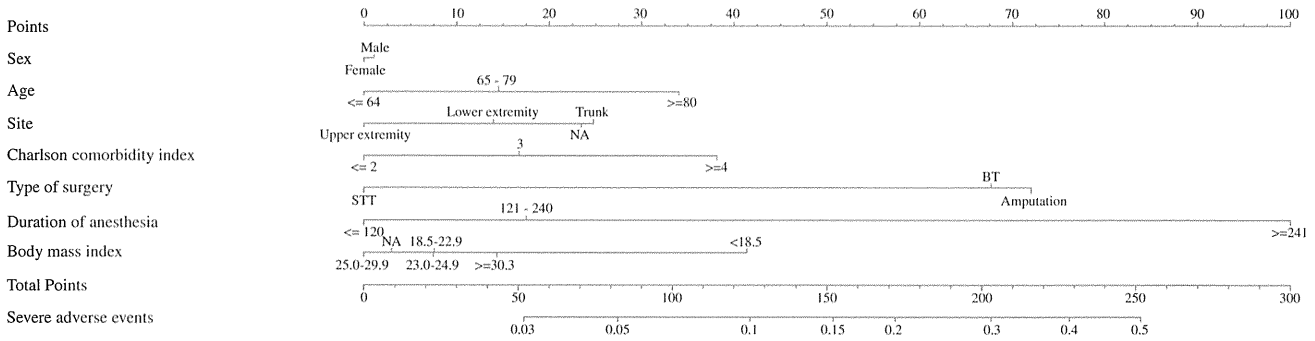

FIG. 1 Nomogram to predict the probability of severe AEs after musculoskeletal tumor surgery. The patient's value for each parameter is plotted on the appropriate scale and *vertical lines* are drawn to the line of points to obtain the corresponding scores. All scores should be summed to obtain the total points score. The total points score on the total points line is plotted and a *vertical line* is drawn down to the *bottom line*. The corresponding value shows the predicted probability of severe AEs after musculoskeletal tumor surgery for the patient. *AEs* adverse events

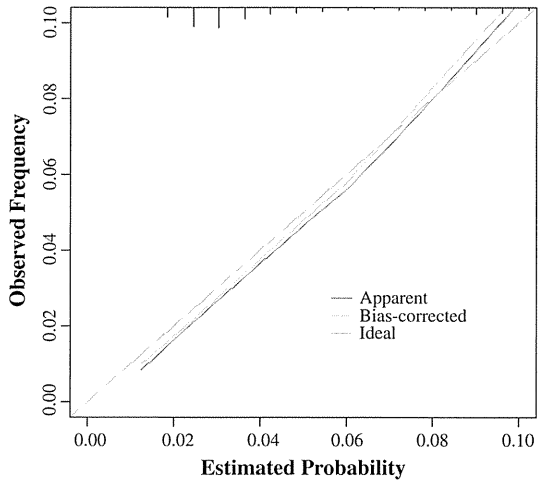

FIG. 2 Calibration plot. The ideal line at 45° (*dashed line*) indicates the ideal nomogram reference line. The apparent line (*dotted line*) shows the calculated data from the dataset. The bias-corrected line (*continuous line*) is an adjusted line by the bootstrap method with 50 resamples

postoperative severe AEs and also developed a nomogram. Presumably, many musculoskeletal oncologists have experienced patients with several severe AEs after surgery and may recognize the population at higher risk of developing severe AEs. To date, however, quantitative evidence to show this tendency has been lacking. Furthermore, our nomogram enables easy calculation of individualized predictions for patient outcomes. Consequently, physicians can recognize the risk for a severe AE before surgery, and provide a more informative explanation to their patients.

The calibration plot (Fig. 2) showed that our nomogram was well-fitted to the observed data. The relatively low incidence of severe AEs (10.7 %) would make it difficult to show a significant association between these variables and severe AEs and develop a nomogram with a standard case series. We overcame this difficulty by using a nationwide database and collecting a large number of contemporary cases from 409 hospitals.

The present study clarified the novel important finding of a relationship between BMI and outcomes. Specifically, the underweight group had significantly worse outcomes than the normal weight group, while the overweight group showed no significance. Although no previous studies have examined the relationship between BMI and surgical outcomes in musculoskeletal tumor surgery, several investigators have documented the impact of BMI on other surgical outcomes. Some studies suggested that obesity conferred an increased risk of postoperative complications in various surgical procedures, such as vascular surgery,[13] gastrectomy,[14,15] pancreaticoduodenectomy,[16] and hepatic resection,[17] while other studies found the opposite result, suggesting that obesity did not necessarily increase the rates of major postoperative complications or death in general surgery [18–20] and orthopedic surgeries, including spinal surgery [21] and total hip arthroplasty.[22] This discrepancy may result from a lack of statistical power in most studies owing to small sample sizes. Recent studies with relatively large sample sizes have demonstrated the worst outcomes in underweight patients and lower mortality in mildly obese patients,[23–26] which is described as the 'obesity paradox'.[24,26] Although better outcomes in obese patients were not noted, the results of the present study were consistent with the previous studies with respect to the worst outcomes in the underweight population. An explanation for the poor outcomes in the underweight population may be related to poor nutritional condition, possibly resulting from chronic disease, cancer-bearing status, or preoperative chemotherapy. Another reason may be that adipose tissue is not only a lipid storage depot, but also biologically produces and secretes adipokines, which may have protective effects in response to injury and tissue repair.[27,28] Our results may reflect the low prevalence of extreme obesity in Japan compared with Western countries. A preoperative

nutritional program for underweight patients may improve outcomes after musculoskeletal tumor surgery.

Our study has several limitations. First, the use of an administrative claims database could have resulted in underestimation or overestimation of comorbidities through incomplete reporting. Second, we were unable to determine AEs after discharge or transfer to another hospital, which may have resulted in underestimation of these outcomes. Third, we were not able to identify several important parameters that may have affected the rates of severe AEs, including histological diagnosis, clinical stage of tumor, severity of preoperative comorbidities, adjuvant chemotherapy and radiotherapy, and some details of surgery. Fourth, it is possible that amputation was performed in sarcoma patients for reasons other than radical tumor resection, such as postoperative deep infection. Although the frequency of such situations is assumed to be rare, the precise number of amputations for tumor resection alone is unknown. Finally, it is possible that individual patients may have been counted more than once in the DPC database, if they initially received inappropriate surgical management at a local hospital that did not participate in the DPC survey and then underwent surgery in a specialized hospital. However, such cases are rare in Japan because there are limited numbers of hospitals specializing in musculoskeletal oncology, and patients are usually referred to a specialized hospital if musculoskeletal sarcoma is suspected.

Despite these limitations, we believe that the present analysis and nomogram based on a large number of patients provide the best evidence on postoperative severe AEs. In addition, the DPC database population is representative of the population in Japan, and includes the majority of patients undergoing musculoskeletal tumor surgery in Japan. The DPC data included approximately 50 % of all hospital admissions in Japan during 2011. According to data from the Nationwide bone and soft tissue tumor registry in Japan, more than 80 % of patients with primary musculoskeletal tumors underwent surgery in university hospitals or cancer treatment centers adopting the DPC system, owing to the rarity of the diseases and the specialized surgical procedures required.

CONCLUSIONS

We have identified independent risk factors for severe AEs after musculoskeletal tumor surgery and developed a nomogram to predict the probability of severe AEs. Underweight, but not overweight or obese, status was significantly associated with increased severe AEs after adjusting for patient background characteristics. In underweight patients, a preoperative nutritional program may improve surgical outcomes after musculoskeletal tumor surgery.

ACKNOWLEDGMENT This study was supported by a Grant-in-Aid for Research on Policy Planning and Evaluation from the Ministry of Health, Labour and Welfare, Japan (Grant No. H22-Policy-031), and by the Funding Program for World-Leading Innovative R&D on Science and Technology (FIRST program) from the Council for Science and Technology Policy, Japan (No. 0301002001001).

DISCLOSURES Koichi Ogura, Hideo Yasunaga, Hiromasa Horiguchi, Kiyohide Fushimi, Sakae Tanaka, and Hirotaka Kawano have declared no conflicts of interest.

REFERENCES

1. Cannon CP, Ballo MT, Zagars GK, et al. Complications of combined modality treatment of primary lower extremity soft-tissue sarcomas. *Cancer*. 2006;107:2455–2461.
2. Damron TA, Wardak Z, Glodny B, Grant W. Risk of venous thromboembolism in bone and soft-tissue sarcoma patients undergoing surgical intervention: a report from prior to the initiation of SCIP measures. *J Surg Oncol*. 2011;103:643–647.
3. Jeys LM, Grimer RJ, Carter SR, Tillman RM. Periprosthetic infection in patients treated for an orthopaedic oncological condition. *J Bone Joint Surg Am*. 2005;87:842–849.
4. Mitchell SY, Lingard EA, Kesteven P, et al. Venous thromboembolism in patients with primary bone or soft-tissue sarcomas. *J Bone Joint Surg Am*. 2007;89:2433–2439.
5. Tuy B, Bhate C, Beebe K, et al. IVC filters may prevent fatal pulmonary embolism in musculoskeletal tumor surgery. *Clin Orthop Relat Res*. 2009;467:239–245.
6. Zeegen EN, Aponte-Tinao LA, Hornicek FJ, et al. Survivorship analysis of 141 modular metallic endoprostheses at early followup. *Clin Orthop Relat Res*. 2004;420:239–250.
7. Chikuda H, Yasunaga H, Horiguchi H, et al. Impact of age and comorbidity burden on mortality and major complications in older adults undergoing orthopaedic surgery: an analysis using the Japanese diagnosis procedure combination database. *BMC Musculoskelet Disord*. 2013;14:173.
8. Kadono Y, Yasunaga H, Horiguchi H, et al. Statistics for orthopedic surgery 2006–2007: data from the Japanese diagnosis procedure combination database. *J Orthop Sci*. 2010;15:162–170.
9. Ogura K, Yasunaga H, Horiguchi H, et al. Incidence and risk factors for pulmonary embolism after primary musculoskeletal tumor surgery. *Clin Orthop Relat Res*. 2013;471:3310–3316.
10. Ogura K, Yasunaga H, Horiguchi H, et al. Impact of hospital volume on postoperative complications and in-hospital mortality after musculoskeletal tumor surgery: analysis of a national administrative database. *J Bone Joint Surg Am*. 2013;95:1684–1691.
11. Charlson ME, Pompei P, Ales KL, MacKenzie CR. A new method of classifying prognostic comorbidity in longitudinal studies: development and validation. *J Chronic Dis*. 1987;40:373–383.
12. World Health Organization. Global database on body mass index. Available from: http://apps.who.int/bmi/index.jsp. Accessed 18 Mar 2014.
13. Chang JK, Calligaro KD, Ryan S, et al. Risk factors associated with infection of lower extremity revascularization: analysis of 365 procedures performed at a teaching hospital. *Ann Vasc Surg*. 2003;17:91–96.
14. Yasunaga H, Horiguchi H, Matsuda S, et al. Body mass index and outcomes following gastrointestinal cancer surgery in Japan. *Br J Surg*. 2013;100:1335–1343.

15. Kodera Y, Ito S, Yamamura Y, et al. Obesity and outcome of distal gastrectomy with D2 lymphadenectomy for carcinoma. *Hepatogastroenterology.* 2004;51:1225–1228.
16. House MG, Fong Y, Arnaoutakis DJ, et al. Preoperative predictors for complications after pancreaticoduodenectomy: impact of BMI and body fat distribution. *J Gastrointest Surg.* 2008;12:270–278.
17. Mathur AK, Ghaferi AA, Osborne NH, et al. Body mass index and adverse perioperative outcomes following hepatic resection. *J Gastrointest Surg.* 2010;14:1285–1291.
18. Blee TH, Belzer GE, Lambert PJ. Obesity: is there an increase in perioperative complications in those undergoing elective colon and rectal resection for carcinoma? *Am Surg.* 2002;68:163–166.
19. Dindo D, Muller MK, Weber M, Clavien PA. Obesity in general elective surgery. *Lancet.* 2003;361:2032–2035.
20. Hawn MT, Bian J, Leeth RR, et al. Impact of obesity on resource utilization for general surgical procedures. *Ann Surg.* 2005;241:821–826; discussion 826–828.
21. Patel N, Bagan B, Vadera S, et al. Obesity and spine surgery: relation to perioperative complications. *J Neurosurg Spine.* 2007;6:291–297.
22. Perka C, Labs K, Muschik M, Buttgereit F. The influence of obesity on perioperative morbidity and mortality in revision total hip arthroplasty. *Arch Orthop Trauma Surg.* 2000;120:267–271.
23. Mullen JT, Davenport DL, Hutter MM, et al. Impact of body mass index on perioperative outcomes in patients undergoing major intra-abdominal cancer surgery. *Ann Surg Oncol.* 2008;15:2164–2172.
24. Davenport DL, Xenos ES, Hosokawa P, et al. The influence of body mass index obesity status on vascular surgery 30-day morbidity and mortality. *J Vasc Surg.* 2009;49:140–147,147 e141; discussion 147.
25. Giles KA, Hamdan AD, Pomposelli FB, et al. Body mass index: surgical site infections and mortality after lower extremity bypass from the National surgical quality improvement program 2005–2007. *Ann Vasc Surg.* 2010;24:48–56.
26. Mullen JT, Moorman DW, Davenport DL. The obesity paradox: body mass index and outcomes in patients undergoing nonbariatric general surgery. *Ann Surg.* 2009;250:166–172.
27. Hotamisligil GS. Inflammation and metabolic disorders. *Nature.* 2006;444:860–867.
28. Odrowaz-Sypniewska G. Markers of pro-inflammatory and prothrombotic state in the diagnosis of metabolic syndrome. *Adv Med Sci.* 2007;52:246–250.

Eccentric Femoral Tunnel Widening in Anatomic Anterior Cruciate Ligament Reconstruction

Shuji Taketomi, M.D., Hiroshi Inui, M.D., Takaki Sanada, M.D., Ryota Yamagami, M.D., Sakae Tanaka, M.D., Ph.D., and Takumi Nakagawa, M.D., Ph.D.

Purpose: The purpose of this study was to retrospectively evaluate femoral tunnel widening (TW) and migration of the femoral tunnel aperture after anatomic anterior cruciate ligament (ACL) reconstructions with hamstring grafts and bone–patellar tendon–bone (BPTB) grafts. **Methods:** Of the 105 consecutive patients who underwent ACL reconstruction, the 52 patients who underwent isolated ACL reconstruction and in whom tunnel measurement could be obtained by computed tomography were included in this study. In 26 patients, double-bundle reconstruction (DBR) of the ACL using hamstring tendons was performed. These patients were compared with 26 patients in whom rectangular tunnel ACL reconstruction using BPTB grafts (BPTBR) was performed. Femoral tunnel aperture positioning and TW were investigated postoperatively using 3-dimensional computed tomographic images, which were performed a week and a year after surgery in all patients. **Results:** In DBR, the average diameter of the anteromedial (AM) femoral tunnel increased by 34.0% in the horizontal direction and 28.2% in the vertical direction, whereas that of the posterolateral (PL) femoral tunnel increased by 58.2% and 73.4%, respectively, at 1 year after surgery compared with 1 week after surgery. The percentage TW value of the PL tunnel was significantly greater than that of the AM tunnel. In BPTBR, the average diameter increased by 22.0% and 17.1%, respectively. The percentage TW value of the PL tunnel in DBR was significantly greater than that of the femoral tunnel in BPTBR. Each tunnel aperture migrated distally ("shallow") in the horizontal direction and high in the vertical direction. AM and PL tunnel apertures in DBR migrated in the vertical direction significantly more than they did in BPTBR. No significant differences between the 2 groups were found in clinical outcomes. **Conclusions:** The femoral PL tunnel aperture in DBR showed significantly more widening than did the AM tunnel aperture in DBR and the femoral tunnel aperture in BPTBR. Also, greater migration of the femoral tunnel aperture in the vertical direction because of TW was observed in DBR than in BPTBR. **Level of Evidence:** Level IV, therapeutic case series.

Tunnel widening (TW) after anterior cruciate ligament (ACL) reconstruction is a well-known phenomenon. Greater TW has been reported in ACL reconstruction using hamstring grafts than in that using bone–patellar tendon–bone (BPTB) grafts.[1-4] The causes of TW are unclear and are presumed to be multifactorial, with biological and mechanical factors. Biological factors include access of the synovial fluid between the graft and the bone that contains osteolytic cytokines.[5] Mechanical factors include a "bungee effect," as longitudinal motion of the graft by extracortical femoral fixation, a "windshield-wiper effect," as transverse motion of the graft, improper graft placement, and accelerated rehabilitation.[6-8] Although TW does not seem to affect the short-term clinical outcome, a general consensus prevails that the presence of expanded tunnels often severely complicates revision ACL reconstruction.[9,10]

Recently, ACL reconstruction has focused on anatomically reconstructing the ligament to restore the original footprint and normal kinematics of the knee. During anatomic ACL reconstruction, the lateral intercondylar ridge is an important topographic landmark to identify the femoral attachment of the ACL.[11-13] In theory, graft placement aligned within native insertion sites, especially the femoral site, could result in the restoration of knee stability and superior clinical outcomes.[14] Nonanatomically positioned femoral bone

From Department of Orthopaedic Surgery (S.T., H.I., T.S., R.Y., S.T.), Faculty of Medicine, The University of Tokyo; and Department of Orthopaedic Surgery (T.N.), Teikyo University School of Medicine, Tokyo, Japan.

The authors report that they have no conflicts of interest in the authorship and publication of this article.

Received September 22, 2013; accepted February 6, 2014.

Address correspondence to Shuji Taketomi, M.D., Department of Orthopaedic Surgery, Faculty of Medicine, The University of Tokyo, 7-3-1 Hongo, Bunkyo-ku, Tokyo 113-0033, Japan. E-mail: takeos-tky@umin.ac.jp

0749-8063/13690/$36.00

http://dx.doi.org/10.1016/j.arthro.2014.02.016

tunnels result in more TW compared with anatomically positioned tunnels.[15,16] Although many authors have described TW, most reports in the literature have not discussed the direction of TW or tunnel aperture migration. If TW and tunnel aperture migration occur after an ACL reconstruction procedure in which the femoral tunnel was placed in the anatomic position, there is a possibility that the femoral tunnel aperture extrudes into a nonanatomic position. Therefore, it is important to know the direction of tunnel aperture migration if it occurs.

Although there are several studies that describe TW after anatomic double-bundle reconstruction (DBR) of the ACL, most of these studies compared DBR with single-bundle ACL reconstruction.[17,18] In contrast, there is no study about TW after anatomic ACL reconstruction using BPTB grafts. Since 2007, we have used a 3-dimensional (3D) fluoroscopy-based navigation system to accurately and reproducibly position the femoral tunnel during anatomic ACL reconstruction using hamstring tendon grafts or BPTB grafts.[19,20] Therefore, we conducted a study comparing femoral TW after anatomic DBR and anatomic ACL reconstruction using a BPTB graft with the objective of placing the femoral tunnel aperture within the native ACL footprint (i.e., posterosuperior to the lateral intercondylar ridge of the femur). Knowledge about TW after anatomic ACL reconstruction using 2 different graft materials is essential for the selection of a graft. Furthermore, knowing the direction of TW after ACL reconstruction could lead to an appropriate tunnel placement in ACL reconstruction. To the best our knowledge, this is the first study comparing femoral TW and migration of the femoral tunnel aperture in anatomic ACL reconstructions using hamstring tendon grafts versus those using BPTB grafts.

The purpose of this study was to retrospectively evaluate femoral TW and migration of the femoral tunnel aperture after anatomic ACL reconstructions using hamstring tendon and BPTB grafts through the use of a 3D computed tomography (CT) model. Our hypothesis was that greater TW and migration of the femoral tunnel aperture would occur in anatomic ACL reconstructions using hamstring grafts than in those using BPTB grafts.

Methods

Patients

Of the 105 consecutive patients on whom ACL reconstruction was performed at our institution between July 2009 and February 2012, 52 patients were included in this study. Inclusion criteria for the study were as follows: (1) history of a DBR ACL reconstruction using hamstring tendon grafts or a rectangular tunnel ACL reconstruction using a BPTB graft (BPTBR), (2) no previous intra-articular ligament reconstruction or osteotomy around the knee joint, (3) absence of posterior cruciate ligament insufficiency or abnormal varus/valgus instability, and (4) existence of a bone bridge between anteromedial (AM) and posterolateral (PL) tunnels seen on CT in cases of DBR (i.e., the tunnels had to be separated by a bridge of bone to allow measurement of each tunnel). There was one patient who did not meet the first inclusion criterion, 19 patients who did not meet the second criterion, one who did not meet the third criterion, and 18 who did not meet the fourth criterion; therefore, a total of 39 patients were excluded. In addition, 2 patients did not give their consent for CT and 11 patients were lost to follow-up. An experienced surgeon participated in all procedures as an operator or first assistant. In 26 of the 52 patients, DBR was performed. These patients were compared with 26 patients in whom BPTBR was performed. Patients in the study included 14 female patients and 38 male patients with a median age of 27 years (range, 16 to 50 years). Grafts were selected by a surgeon who took into consideration the activity of patients, the types of sports they may be involved in, and patient preference. BPTB grafts were selected primarily for young male or collision/contact athletes, whereas hamstring grafts were selected for the others during the study period. Patient information is summarized in Table 1. The institutional review board at our institution approved this retrospective study. Patients and their families were informed that data from their cases would be submitted for publication, and they all provided consent.

Table 1. Preoperative Patient Information

	DBR	BPTBR	*P* value
Number of patients	26	26	
Gender (female/male)	12/14	2/24	.002*
Age (years)	31 (18-50)	26 (16-47)	.012*
Body height (cm)	167 ± 9	171 ± 5	.015*
Body weight (kg)	64 ± 12	70 ± 15	.047*
Body mass index (kg/m^2)	22.8 ± 2.9	23.7 ± 4.2	.191
Tegner activity scale	7 (3-9)	8 (5-10)	.053

NOTE. Data are given as means ± standard deviations or medians (range).

*Indicates a statistical significance between the 2 groups with $P < .05$.

Surgical Technique of DBR

ACL reconstruction was arthroscopically performed using a 3D fluoroscopy-based navigation system to place the 2 femoral tunnels, as described previously.[19,21] Briefly, the autologous hamstring tendons were harvested and the doubled grafts were looped over EndoButton CLs (Smith & Nephew, Andover, MA). The distal free ends of the grafts were armed with No. 3 Ethibond (Somerville, NJ) sutures using a whipstitch technique. The femoral insertion site for each

bundle was determined by monitoring the bony landmarks[22,23] (i.e., the lateral intercondylar ridge and the lateral bifurcate ridge) both by the arthroscopic view and on the navigation screen (StealthStation TRIA Plus, Medtronic, Minneapolis, MN). The priority for creating the femoral tunnels was to position the femoral tunnel apertures within the femoral footprint of the ACL. Two guidewires for the femoral tunnel were placed through a far AM portal[24] while referencing the navigation computer screen and were then overdrilled to an adequate length using a cannulated drill. Next, the lateral femoral cortex was drilled through using an EndoButton drill (Smith & Nephew, Andover, MA). On the tibial side, 2 guidewires were positioned and overdrilled to the full length using a cannulated drill. The tibial insertion site was arthroscopically determined in reference to the ACL remnant, the medial tibial eminence, the anterior horn of the lateral meniscus, the intermeniscal ligament, and the posterior cruciate ligament.[25] The tibial tunnels were placed in the center of the AM and PL footprints. After creating 2 femoral tunnels and 2 tibial tunnels, both grafts were passed through and the EndoButton loop was flipped outside the femoral cortex in the usual manner. The desired length of the graft within the femoral tunnel was 14 to 18 mm. Tibial fixation of the hamstring autografts was accomplished over a suture after fixation with a fully threaded 6.5-mm cancellous screw and washer (Meira, Nagoya, Japan). The AM bundle graft was fixed at 60° of knee flexion and the PL bundle was fixed at full knee extension.

Surgical Technique of BPTBR

ACL reconstruction with BPTB grafts was performed using the same navigation system. Autologous BPTB grafts were 10 mm in width and were harvested with bone plugs at both ends from the central portion of the patellar tendon. The femoral bone plug for a rectangular tunnel was usually 5 × 10 × 15 mm as described by Shino et al.[26] It was connected to an EndoButton using No. 5 and No. 2 FiberWire (Arthrex, Naples, FL). The femoral insertion site was determined in the same manner as in the hamstring reconstruction procedure. Two parallel guidewires for the femoral tunnel were then placed and overdrilled for an appropriate length using a 5-mm cannulated drill.[26] The 2 tunnels were interconnected using a dilator (Smith & Nephew, Andover, MA) and the lateral femoral cortex was drilled through the center of the 2 tunnels using an EndoButton drill. On the tibial side, 2 parallel guidewires were positioned and overdrilled the full length using a cannulated drill, and the 2 tunnels were interconnected using a dilator (Smith & Nephew, Andover, MA). The tibial insertion site was determined in the same manner as in the DBR procedure. After creating a femoral tunnel and a tibial tunnel, the BPTB graft was passed through, and the EndoButton loop was flipped outside the femoral cortex in the usual manner. The bone plug was set far enough into the femoral tunnel that the ligament end of the graft was inset 1 mm into the femoral tunnel to avoid protrusion of the bone plug from the femoral tunnel. Tibial fixation of the BPTB graft was accomplished in the same manner as in the DBR procedure, and the BPTB graft was fixed at full knee extension.

Postoperative Rehabilitation

The knee was not immobilized but was protected for 5 weeks with a functional brace. Active and assisted range of motion exercises were started immediately after surgery. Partial weight bearing was allowed 2 days after surgery and full weight bearing was allowed at 1 week. Running was allowed at 4 months followed by a return to previous sporting activity at an average of 8 to 9 months after surgery.

Computed Tomographic Evaluation

A 3D computed tomographic scan of the operated knee was obtained a week and a year after surgery for all patients, using a helical high-speed Aquilion 64 or Aquilion ONE (Toshiba Medical Systems, Tochigi, Japan) CT machine. The ZIOSTATION software package (Ziosoft, Tokyo, Japan) was used for 3D reconstruction of the operated knee. The tibia, patella, and medial femoral condyle were removed from the 3D model because it was necessary to visualize the lateral wall of the intercondylar notch. A true medial view of the femur was established by superimposing the posterior aspects of the femoral condyles. All measurements were made on the surface of the lateral wall of the intercondylar notch completely from an orthogonal projection to the angle of the surface being measured to ensure accuracy. An orthopaedic surgeon (S.T.) conducted the CT measurement.

Measurement of the Femoral Tunnel Diameter

The horizontal diameter (D_H) of the femoral tunnel was defined as the width of the femoral tunnel aperture along the Blumensaat line and the vertical diameter (D_V) was defined as the height of the femoral tunnel aperture perpendicular to the Blumensaat line (Fig 1). The tunnel diameter measured 1 week after surgery was used as the baseline measurement, which was compared with the diameter measured at the 1-year postoperative follow-up. A percentage change in the diameter between the 2 periods was defined as the percentage TW value.

Measurement of the Femoral Tunnel Aperture Positioning

Morphometric assessment of femoral tunnel positioning was performed according to the quadrant

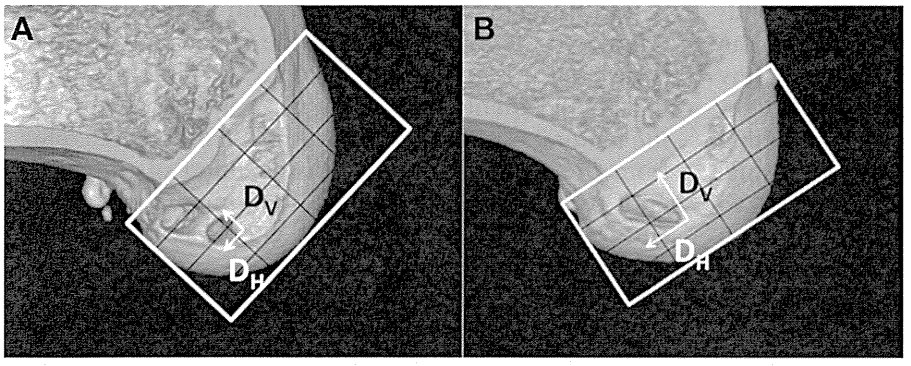

Fig 1. Measurements of the horizontal diameter (D_H) and the vertical diameter (D_V) of the femoral tunnel aperture on a grid of the quadrant method described by Bernard et al.[27] (A) Measurements at 1 week postoperatively for 2 femoral tunnels in double-bundle ACL reconstruction using hamstring tendon grafts. (B) Measurements of the horizontal diameter (D_H) and the vertical diameter (D_V) for rectangular femoral tunnel in ACL reconstruction using BPTB grafts.

technique as described by Bernard et al.[27] The total sagittal diameter of the lateral condyle along the Blumensaat line (D) and the maximum lateral intercondylar notch height (H) were measured using the 3D computed tomographic image. The distance from the center of the femoral tunnel aperture to the most posterior subchondral contour of the lateral femoral condyle (d), and the distance from the center of each tunnel for hamstring tendon graft to Blumensaat's line (h) was measured (Fig 2A). For the rectangular tunnel for the BPTB grafts, the center of the ellipse by which the rectangular tunnel aperture was approximated was defined as the center of the femoral tunnel for the BPTB graft (Fig 2B). The length of distance d as a partial distance of D and the height of the distance h as a partial distance of H were expressed in percentages, such as d/D% and h/H%, respectively.

Clinical Evaluation

Clinical assessment was performed 1 year after surgery, corresponding to the period of computed tomographic assessment. All patients were subjectively evaluated using the Lysholm score.[28] Anterior knee stability was quantitatively assessed using a KT-2000 arthrometer (MEDmetric, San Diego, CA). Reconstructed and contralateral knees were measured with a 134-N anterior force applied to the proximal tibia at 20° of knee flexion. The side-to-side difference in anterior translation was used as a representative indicator of restored knee stability. The pivot shift test was graded as negative, glide, clunk, or gross to determine rotational stability.[29] The range of motion of the reconstructed and contralateral knees were evaluated.

Statistical Analysis

Statistical analysis was performed using the EXCEL statistics 2012 software package for Microsoft Windows (SSRI, Tokyo, Japan). Patient parameters were compared using the Student *t* test and the Mann-Whitney *U* test. Radiographic parameters were compared using the Student *t* test. Clinical outcomes were compared with the Student *t* test and the χ-square test. The statistical significance level was set at $P < .05$. One orthopaedic surgeon (S.T.) previously performed a

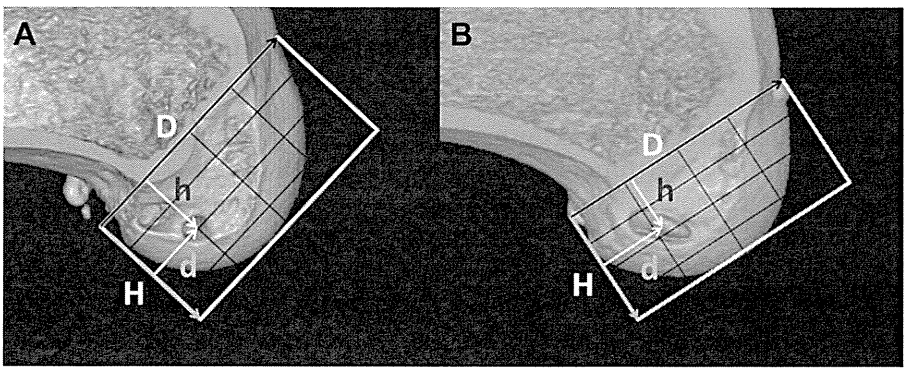

Fig 2. Measurements of femoral tunnel positioning using the quadrant method described by Bernard et al.[27] (A) Measurements at 1 week postoperatively for the center of 2 femoral tunnels in double-bundle ACL reconstruction using hamstring tendon grafts. (B) Measurements of femoral tunnel positioning for the rectangular femoral socket in ACL reconstruction using BPTB grafts. D, total sagittal diameter of the lateral condyle along the Blumensaat line; d, distance from the center of the femoral tunnel aperture to the most posterior subchondral contour of the lateral femoral condyle; H, maximum lateral intercondylar notch height; h, distance from the center of the tunnel aperture to Blumensaat's line.

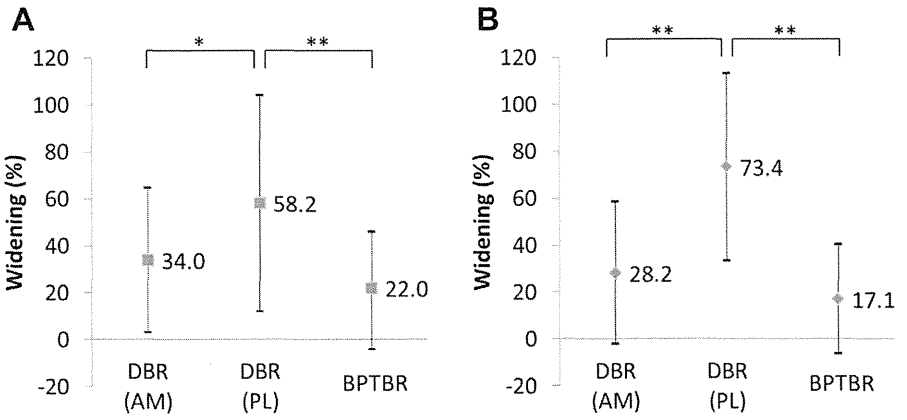

Fig 3. Graphs showing the mean widening of the femoral tunnel aperture. (A) The horizontal direction. (B) The vertical direction. The error bars denote the standard deviation. *indicates a statistical significance between the 3 groups with $P < .05$. **indicates a statistical significance between the 2 groups with $P < .001$. AM, anteromedial; DBR, double-bundle reconstruction; PL, posterolateral.

pilot study of 10 patients. In this study, the mean difference of the femoral tunnel aperture location using the quadrant method between 2 time points was 3.3%, and standard deviation was 7.1% and 7.7% at 1 week and 1 year postoperatively, respectively. A previous power analysis indicated that a sample size of at least 26 patients per group was necessary to detect an intergroup difference in the radiographic parameters with an alpha of .05 and a power of 80%. Intraobserver reliability for the radiographic parameters was represented by the intraclass correlation coefficients. A period of 4 weeks elapsed between test and retest measurements. The intraclass correlation coefficients in the pilot study were 0.973 for TW and 0.949 for tunnel location.

Results

TW of the Femoral Tunnel Apertures

Postoperative femoral TW is described in Fig 3. Data in text are given as mean ± standard deviation. The actual values of TW (in millimeters) are also described after the percentage increased. In DBR, the average diameter of the AM femoral tunnel aperture increased by 34.0% ± 30.7% (1.8 ± 1.6 mm) in the horizontal direction and 28.2% ± 30.2% (1.3 ± 1.4 mm) in the vertical direction, whereas the average diameter of the PL increased by 58.2% ± 46.0% (2.8 ± 2.2 mm) and 73.4% ± 39.8% (3.1 ± 1.7 mm), respectively, at 1 year after surgery compared with 1 week after surgery. The percentage TW value of PL tunnel apertures was significantly greater than that of AM tunnels ($P < .05$ in the horizontal direction; $P < .001$ in the vertical direction). In BPTBR, the average diameter of the femoral tunnel aperture increased by 22.0% ± 26.1% (1.8 ± 2.1 mm) in the horizontal direction and 17.1% ± 23.4% (1.4 ± 1.9 mm) in the vertical direction. The percentage TW value of PL tunnel apertures in DBR was significantly greater than that of the femoral tunnel apertures in BPTBR ($P < .001$ in the horizontal direction; $P < .001$ in the vertical direction), whereas there were no significant differences between the percentage TW value of AM tunnel apertures in DBR and that of femoral tunnel apertures in BPTBR ($P = .14$ in the horizontal direction; $P = .15$ in the vertical direction).

Tunnel Migration of the Femoral Tunnel Apertures

The average center of the femoral tunnel aperture at 1 week after surgery and at 1 year after surgery are described in Table 2. The tunnel aperture positions differed significantly among BPTBR, AM tunnels in DBR, and PL tunnels in DBR on computed tomographic images. Each tunnel aperture migrated distally ("shallow") in the horizontal direction and high in the vertical direction 1 year after surgery. The AM tunnel aperture and the PL tunnel aperture in DBR migrated in the vertical direction significantly more than the tunnel aperture in BPTBR ($P < .001$, $P < .001$, respectively).

Clinical Evaluation

Data in text are given as means ± standard deviations. The postoperative mean Lysholm score was 97.6 ± 3.4 points in DBR and 97.6 ± 3.3 points in BPTBR. The postoperative side-to-side difference in anterior translation measured with the KT-2000 arthrometer averaged 0.1 ± 1.0 mm in DBR and 0.2 ± 1.6 mm in BPTBR. The postoperative pivot shift test produced negative or glide results in all patients (100%) of both groups. With respect to the range of motion of the knee, loss of extension of greater than 5° compared with the contralateral knee was not observed in either group, whereas loss of flexion of greater than 5° compared with the contralateral knee was observed in 1 patient (4%) from each group. No significant difference between the 2 groups was found in all clinical outcomes.

Discussion

This study revealed 3 important findings. First was that the femoral PL tunnel showed significantly greater widening than the AM tunnel in anatomic DBR. Most previous studies describing TW in DBR did not show

Table 2. Center of Femoral Tunnel Apertures and Migration

	1 Week After Surgery	1 Year After Surgery	*P* Value	Migration	
AM					
d/D(%)	21.9 ± 3.6	24.2 ± 3.4	.004	2.3	
h/H(%)	36.2 ± 6.6	27.4 ± 8.2	<.001	−8.8	
PL					
d/D(%)	32.9 ± 5.9	35.2 ± 4.3	.001	2.3	
h/H(%)	61.1 ± 5.9	53.3 ± 4.6	<.001	−7.8	*
BPTBR					
d/D(%)	27.9 ± 5.7	31.4 ± 5.0	<.001	3.5	*
h/H(%)	50.1 ± 7.3	47.3 ± 7.9	.002	−2.8	

NOTE. Data are expressed as means ± standard deviations.

d/D, center of the tunnel aperture in the horizontal direction from deep; h/H, center of the tunnel aperture in the vertical direction from the Blumensaat' line.

*Indicates a statistical significance between the 2 groups with $P < .001$.

differences of TW between the AM and PL tunnels,[18,30,31] whereas Siebold et al.[32] also observed the higher femoral TW for the PL bundle, which would support the findings in the current study. We have considered the possible reasons why the PL tunnel aperture expanded to a greater extent than the AM tunnel aperture in DBR. One of the reasons is that the AM and PL bundles have different functions, and the PL bundle is associated with a greater change in tension with knee motion.[33-36] This resulted in more extensive motion of the PL graft within the tunnel, and a longer time was required for bone-to-graft healing. The other reason is that although the AM tunnel aperture was surrounded by superior and posterior articular hard subchondral bone and the PL graft, the PL tunnel aperture was surrounded by only posterior articular hard subchondral bone and the AM graft. Therefore, the PL graft had space for expansion.

Second was that greater TW was observed in anatomic ACL reconstruction using hamstring tendon grafts than in BPTBR, especially in the PL tunnel. Although widening of the AM tunnel in DBR was greater than TW in BPTBR, there was no significant difference between AM TW in DBR and TW in BPTBR. Conversely, greater widening of the PL tunnel was observed in DBR than in BPTBR. Although greater TW has been reported in conventional single-bundle ACL reconstruction using hamstring grafts than in that using BPTB grafts,[1-4] there has been no report that compared femoral TW between anatomic ACL reconstructions with hamstring tendon grafts and those using BPTB grafts. We confirmed greater TW in ACL reconstruction using hamstring tendon grafts when anatomic ACL reconstruction was performed with the objective of placing the femoral tunnel aperture within the native ACL footprint (i.e., posterosuperior to the lateral intercondylar ridge). An explanation for smaller TW in BPTBR compared with DBR was simple and clear. In BPTBR, bone-to-graft healing was achieved faster and more securely compared with that achieved with DBR, which resulted in smaller TW in BPTBR.[37] The soft tissue graft length in the tunnel may affect TW. According to a biomechanical study, optimal strength and stiffness of the reconstructed ACL were achieved with 17-mm grafts.[38] In contrast, the relation between the graft length in the tunnel and TW is still unknown. Meanwhile, femoral TW in BPTBR was not so great but did occur because of 2 possible causes. First, a suspension device was used for femoral fixation; consequently, a little motion of the graft within the femoral tunnel occurred.[6,7] Second, the bone plug was set far enough into the femoral tunnel that the ligament end of the graft was inset 1 mm into the femoral tunnel, and as a result a little "windshield-wiper effect" as transverse motion of the graft might occur.

The other important finding of the current study, which has not been reported previously, was that greater migration of the femoral tunnel aperture because of TW was observed in DBR than was seen in BPTBR. This study revealed that the femoral tunnel aperture did not undergo circumferential widening but expanded in a particular direction after ACL reconstruction. As a result, the center of the femoral tunnel aperture migrated. The results of the current study showed that the AM and PL tunnel apertures in DBR migrated mainly in the vertical direction. Surgeons need to take into account the fact that eccentric TW occurs after DBR. We believe that this phenomenon will contribute to further development of anatomic ACL reconstruction.

Most studies of TW comparing extracortical fixation using the suspensory device and other fixation methods showed that greater TW was associated with the use of the suspensory device.[9,39] Buelow et al.[39] reported that extracortical fixation using the EndoButton resulted in greater TW compared with aperture fixation using the interference screw. The results of the current study may be associated with the use of the EndoButton. There are very few studies of TW comparing suspensory fixation and other implants in anatomic DBR or BPTBR. Further

studies are required in the future to address whether aperture fixation decreases TW in anatomic ACL reconstruction.

Clinical outcomes of the current study showed good results after ACL reconstruction and no difference between DBR and BPTBR. It indicated that the grafts in both DBR and BPTBR were clinically functional. However, from the results of this study, it was not known whether TW and tunnel migration affect clinical outcome after anatomic ACL reconstruction. The number of patients involved this study was too small to clarify effects of TW or tunnel migration on clinical outcomes after anatomic ACL reconstruction.

There were some strong points of this study. First, the same surgical method was used for both DBR and BPTBR, such as femoral tunnel positioning and use of fixation devices, whereas in previous studies comparing TW between ACL reconstruction using hamstring tendon grafts and those using BPTB grafts, different surgical methods were used. Second, we used 3D computed tomographic images to evaluate the position of the femoral tunnel aperture. Computed tomographic images are recommended instead of plain radiographs for the postoperative evaluation of tunnel positions in ACL reconstruction procedures.[40] A 3D computed tomographic scan model quadrant method has been reported as reliable in measuring the location of femoral tunnels after ACL reconstruction.[41] We applied this method to evaluate femoral TW and the direction of femoral aperture migration.

Limitations

There were several limitations to this study. First, the current study did not analyze effects of tunnel migration or TW on clinical outcomes after ACL reconstruction, as previously mentioned. Future studies involving a large number of patients are needed to clarify whether these factors influence clinical results after ACL reconstruction. Second, this was a retrospective study with a relatively small number of patients. There were certain dissimilarities between the 2 groups, such as age or sex, because grafts were selected by each surgeon according to patient activity, participation in sports, or patient preference. It is likely that there were differences in bone mineral density (BMD) between the groups because BMD depends on multiple factors such as sex, age, and activity. Differences in BMD between the groups may affect the results of this study. However, according to Meller et al.,[42] there was no correlation between TW and BMD in an animal model of ACL reconstruction. We consider that differences in graft choice rather than the dissimilarities in patient profiles impacted the results of this study. Third, we used 3D computed tomographic images to evaluate TW instead of multiplanar reconstruction CT. Multiplanar CT is more suitable to evaluate TW; however, the focus of this study was to evaluate migration of the femoral tunnel aperture. As previously mentioned, a 3D computed tomographic scan model quadrant method has been reported as reliable to measure the location of femoral tunnels after ACL reconstruction. Therefore, we used a 3D computed tomographic scan model to evaluate both TW and migration of femoral tunnel aperture in this study. Another option exists in which measurement of the tunnel diameter along the tunnel aperture axis can be performed to obtain the diameter of the elliptic tunnel. Because evaluation of eccentric TW was a high priority, the use of the same rectangular coordinates was chosen to measure both TW and migration of tunnel aperture. Fourth, tibial TW or tunnel migration was not evaluated in this study, whereas femoral TW and tunnel aperture migration were evaluated. Whether a similar migration phenomenon occurs with tibial tunnels should be clarified in future studies. Fifth, in DBR, patients were excluded if a bone bridge between the AM and PL tunnels could not be identified on 3D CT. It was difficult to evaluate each tunnel diameter when 2 tunnels communicated with each other. Finally, a short follow-up period and large variability in the results were also limitations of this study.

Conclusions

The femoral PL tunnel aperture in DBR showed significantly greater widening than did the AM tunnel aperture in DBR and the femoral tunnel aperture in BPTBR. Also, migration of the femoral tunnel aperture in the vertical direction because of TW was greater in DBR than in BPTBR.

References

1. Clatworthy MG, Annear P, Bulow JU, Bartlett RJ. Tunnel widening in anterior cruciate ligament reconstruction: A prospective evaluation of hamstring and patella tendon grafts. *Knee Surg Sports Traumatol Arthrosc* 1999;7:138-145.
2. Webster KE, Feller JA, Hameister KA. Bone tunnel enlargement following anterior cruciate ligament reconstruction: A randomised comparison of hamstring and patellar tendon grafts with 2-year follow-up. *Knee Surg Sports Traumatol Arthrosc* 2001;92:86-91.
3. Aglietti P, Giron F, Buzzi R, Biddau F, Sasso F. Anterior cruciate ligament reconstruction: Bone-patellar tendon-bone compared with double semitendinosus and gracilis tendon grafts. A prospective, randomized clinical trial. *J Bone Joint Surg Am* 2004;86:2143-2155.
4. Hersekli MA, Akpinar S, Ozalay M, et al. Tunnel enlargement after arthroscopic anterior cruciate ligament reconstruction: Comparison of bone-patellar tendon-bone and hamstring autografts. *Adv Ther* 2004;21:123-131.
5. Darabos N, Haspl M, Moser C, Darabos A, Bartolek D, Groenemeyer D. Intraarticular application of autologous conditioned serum (ACS) reduces bone tunnel widening after ACL reconstructive surgery in a randomized

controlled trial. *Knee Surg Sports Traumatol Arthrosc* 2011;19(suppl 1):S36-S46.
6. Baumfeld JA, Diduch DR, Rubino LJ, et al. Tunnel widening following anterior cruciate ligament reconstruction using hamstring autograft: A comparison between double cross-pin and suspensory graft fixation. *Knee Surg Sports Traumatol Arthrosc* 2008;16:1108-1113.
7. Sabat D, Kundu K, Arora S, Kumar V. Tunnel widening after anterior cruciate ligament reconstruction: A prospective randomized computed tomography–based study comparing 2 different femoral fixation methods for hamstring graft. *Arthroscopy* 2011;27:776-783.
8. Höher J, Möller HD, Fu FH. Bone tunnel enlargement after anterior cruciate ligament reconstruction: Fact or fiction? *Knee Surg Sports Traumatol Arthrosc* 1998;6: 231-240.
9. Fauno P, Kaalund S. Tunnel widening after hamstring anterior cruciate ligament reconstruction is influenced by the type of graft fixation used: A prospective randomized study. *Arthroscopy* 2005;21:1337-1341.
10. Wilson TC, Kantaras A, Atay A, Johnson DL. Tunnel enlargement after anterior cruciate ligament surgery. *Am J Sports Med* 2004;32:543-549.
11. Colombet P, Robinson J, Christel P, et al. Morphology of anterior cruciate ligament attachments for anatomic reconstruction: A cadaveric dissection and radiographic study. *Arthroscopy* 2006;22:984-992.
12. Giron F, Cuomo P, Aglietti P, Bull A, Amis A. Femoral attachment of the anterior cruciate ligament. *Knee Surg Sports Traumatol Arthrosc* 2006;14:250-256.
13. Shino K, Suzuki T, Iwahashi T, et al. The resident's ridge as an arthroscopic landmark for anatomical femoral tunnel drilling in ACL reconstruction. *Knee Surg Sports Traumatol Arthrosc* 2010;18:1164-1168.
14. Musahl V, Plakseychuk A, VanScyoc A, et al. Varying femoral tunnels between the anatomical footprint and isometric positions: Effect on kinematics of the anterior cruciate ligament-reconstructed knee. *Am J Sports Med* 2005;33:712-718.
15. Chhabra A, Kline AJ, Nilles KM, Harner CD. Tunnel expansion after anterior cruciate ligament reconstruction with autogenous hamstrings: A comparison of the medial portal and transtibial techniques. *Arthroscopy* 2006;22: 1107-1112.
16. Segawa H, Omori G, Tomita S, Koga Y. Bone tunnel enlargement after anterior cruciate ligament reconstruction using hamstring tendons. *Knee Surg Sports Traumatol Arthrosc* 2001;9:206-210.
17. Kawaguchi Y, Kondo E, Kitamura N, Kai S, Inoue M, Yasuda K. Comparisons of femoral tunnel enlargement in 169 patients between single-bundle and anatomic double-bundle anterior cruciate ligament reconstructions with hamstring tendon grafts. *Knee Surg Sports Traumatol Arthrosc* 2011;19:1249-1257.
18. Järvelä T, Moisala AS, Paakkala T, Paakkala A. Tunnel enlargement after double-bundle anterior cruciate ligament reconstruction: A prospective, randomized study. *Arthroscopy* 2008;24:1349-1357.
19. Nakagawa T, Takeda H, Nakajima K, et al. Intraoperative 3-dimensional imaging-based navigation-assisted anatomic double-bundle anterior cruciate ligament reconstruction. *Arthroscopy* 2008;24:1161-1167.
20. Taketomi S, Inui H, Nakamura K, et al. Three-dimensional fluoroscopic navigation guidance for femoral tunnel creation in revision anterior cruciate ligament reconstruction. *Arthrosc Tech* 2012;1:e95-e99.
21. Taketomi S, Nakagawa T, Takeda H, et al. Anatomical placement of double femoral tunnels in anterior cruciate ligament reconstruction: Anteromedial tunnel first or posterolateral tunnel first? *Knee Surg Sports Traumatol Arthrosc* 2011;19:424-431.
22. Ferretti M, Ekdahl M, Shen W, Fu F. Osseous landmarks of the femoral attachment of the anterior cruciate ligament: an anatomic study. *Arthroscopy* 2007;23:1218-1225.
23. Fu F, Jordan S. The lateral intercondylar ridge—a key to anatomic anterior cruciate ligament reconstruction. *J Bone Joint Surg Am* 2007;89:2103-2104.
24. Shino K, Horibe S, Hamada M, et al. Allograft anterior cruciate ligament reconstruction. *Tech Knee Surg* 2002;1: 78-85.
25. Ferretti M, Doca D, Ingham SM, Cohen M, Fu FH. Bony and soft tissue landmarks of the ACL tibial insertion site: An anatomical study. *Knee Surg Sports Traumatol Arthrosc* 2012;20:62-68.
26. Shino K, Nakata K, Nakamura N, et al. Rectangular tunnel double-bundle anterior cruciate ligament reconstruction with bone-patellar tendon-bone graft to mimic natural fiber arrangement. *Arthroscopy* 2008;24:1178-1183.
27. Bernard M, Hertel P, Hornung H, Cierpinski T. Femoral insertion of the ACL. Radiographic quadrant method. *Am J Knee Surg* 1997;10:14-21.
28. Lysholm J, Gillquist J. Evaluation of knee ligament surgery results with special emphasis on use of a scoring scale. *Am J Sports Med* 1982;10:150-154.
29. Galway H, MacIntosh D. The lateral pivot shift: A symptom and sign of anterior cruciate ligament insufficiency. *Clin Orthop Relat Res* 1980;147:45-50.
30. Lee YS, Lee SW, Nam SW, et al. Analysis of tunnel widening after double-bundle ACL reconstruction. *Knee Surg Sports Traumatol Arthrosc* 2012;20:2243-2250.
31. Siebold R. Observations on bone tunnel enlargement after double-bundle anterior cruciate ligament reconstruction. *Arthroscopy* 2007;23:291-298.
32. Siebold R, Cafaltzis K. Differentiation between intraoperative and postoperative bone tunnel widening and communication in double-bundle anterior cruciate ligament reconstruction: A prospective study. *Arthroscopy* 2010;26:1066-1073.
33. Amis A, Dawkins G. Functional anatomy of the anterior cruciate ligament. Fibre bundle actions related to ligament replacements and injuries. *J Bone Joint Surg Br* 1991;73: 260-267.
34. Girgis FG, Marshall JL, Monajem A. The cruciate ligaments of the knee joint. Anatomical, functional and experimental analysis. *Clin Orthop Relat Res* 1975;106: 216-231.
35. Kurosawa H, Yamakoshi K, Yasuda K, Sasaki T. Simultaneous measurement of changes in length of the cruciate ligaments during knee motion. *Clin Orthop Relat Res* 1991;265:233-240.

36. Yasuda K, Ichiyama H, Kondo E, Miyatake S, Inoue M, Tanabe Y. An in vivo biomechanical study on the tension-versus-knee flexion angle curves of 2 grafts in anatomic double-bundle anterior cruciate ligament reconstruction: Effects of initial tension and internal tibial rotation. *Arthroscopy* 2008;24:276-284.
37. Suzuki T, Shino K, Nakagawa S, et al. Early integration of a bone plug in the femoral tunnel in rectangular tunnel ACL reconstruction with a bone-patellar tendon-bone graft: A prospective computed tomography analysis. *Knee Surg Sports Traumatol Arthrosc* 2011;19(suppl 1):S29-S35.
38. Yuan F, Zhou W, Cai J, Zhao J, Huangfu X, Yin F. Optimal graft length for anterior cruciate ligament reconstruction: A biomechanical study in beagles. *Orthopedics* 2013;36: e588-e592.
39. Buelow JU, Siebold R, Ellermann A. A prospective evaluation of tunnel enlargement in anterior cruciate ligament reconstruction with hamstrings: Extracortical versus anatomical fixation. *Knee Surg Sports Traumatol Arthrosc* 2002;10:80-85.
40. Hoser C, Tecklenburg K, Kuenzel KH, Fink C. Postoperative evaluation of femoral tunnel position in ACL reconstruction: Plain radiography versus computed tomography. *Knee Surg Sports Traumatol Arthrosc* 2005;13: 256-262.
41. Lertwanich P, Martins CA, Asai S, Ingham SJ, Smolinski P, Fu FH. Anterior cruciate ligament tunnel position measurement reliability on 3-dimensional reconstructed computed tomography. *Arthroscopy* 2011;27:391-398.
42. Meller R, Neddermann A, Willbold E, et al. The relation between tunnel widening and bone mineral density after anterior cruciate ligament reconstruction: An experimental study in sheep. *Arthroscopy* 2010;26:481-487.

nature medicine

Pathogenic conversion of Foxp3$^+$ T cells into T_H17 cells in autoimmune arthritis

Noriko Komatsu[1,2], Kazuo Okamoto[1,2], Shinichiro Sawa[1,2], Tomoki Nakashima[2–4], Masatsugu Oh-hora[3–5], Tatsuhiko Kodama[6], Sakae Tanaka[7], Jeffrey A Bluestone[8] & Hiroshi Takayanagi[1,2,9]

Autoimmune diseases often result from an imbalance between regulatory T (T_{reg}) cells and interleukin-17 (IL-17)-producing T helper (T_H17) cells; the origin of the latter cells remains largely unknown. Foxp3 is indispensable for the suppressive function of T_{reg} cells, but the stability of Foxp3 has been under debate. Here we show that T_H17 cells originating from Foxp3$^+$ T cells have a key role in the pathogenesis of autoimmune arthritis. Under arthritic conditions, CD25^{lo}Foxp3$^+$CD4$^+$ T cells lose Foxp3 expression (herein called exFoxp3 cells) and undergo transdifferentiation into T_H17 cells. Fate mapping analysis showed that IL-17–expressing exFoxp3 T (exFoxp3 T_H17) cells accumulated in inflamed joints. The conversion of Foxp3$^+$CD4$^+$ T cells to T_H17 cells was mediated by synovial fibroblast-derived IL-6. These exFoxp3 T_H17 cells were more potent osteoclastogenic T cells than were naive CD4$^+$ T cell–derived T_H17 cells. Notably, exFoxp3 T_H17 cells were characterized by the expression of Sox4, chemokine (C-C motif) receptor 6 (CCR6), chemokine (C-C motif) ligand 20 (CCL20), IL-23 receptor (IL-23R) and receptor activator of NF-κB ligand (RANKL, also called TNFSF11). Adoptive transfer of autoreactive, antigen-experienced CD25^{lo}Foxp3$^+$CD4$^+$ T cells into mice followed by secondary immunization with collagen accelerated the onset and increased the severity of arthritis and was associated with the loss of Foxp3 expression in the majority of transferred T cells. We observed IL-17$^+$Foxp3$^+$ T cells in the synovium of subjects with active rheumatoid arthritis (RA), which suggests that plastic Foxp3$^+$ T cells contribute to the pathogenesis of RA. These findings establish the pathological importance of Foxp3 instability in the generation of pathogenic T_H17 cells in autoimmunity.

Foxp3-expressing T_{reg} cells have an essential role in suppressing immune responses[1–5]. Mice deficient in Foxp3 develop fatal autoimmune disease[3,4], and continuous expression of Foxp3 throughout life prevents autoimmunity[6]. Thus, the stability of Foxp3 expression influences the balance between tolerance and autoimmunity, as well as the efficacy of T_{reg} cell–based therapies. The instability of Foxp3 may underlie the pathogenesis of autoimmune diabetes and lethal protozoa infection[7–9], but this concept has been challenged by a report showing that Foxp3 expression is stable in *in vivo* disease models, including autoimmune arthritis[10]. A debate has arisen as to whether the plasticity of Foxp3-expressing T_{reg} cells is pathologically relevant. T_{reg} cell development and function are regulated by IL-2, which binds to the receptor complex containing IL-2Rα (also called CD25). It was recently shown that Foxp3$^+$ cells are comprised of Foxp3-stable CD25^{hi} and Foxp3-unstable CD25^{lo} populations[11,12], the former of which is composed of *bona fide* T_{reg} cells with sustained Foxp3 expression[11]. However, the pathological importance of the latter Foxp3-unstable CD25^{lo} population remains unclear.

RESULTS

T_H17 cells arise from CD25^{lo}Foxp3$^+$ T cells in arthritis

To evaluate the *in vivo* stability of Foxp3 in Foxp3$^+$CD4$^+$ T cells and its impact on collagen-induced arthritis (CIA), we adoptively transferred CD25^{hi}Foxp3$^+$CD4$^+$ or CD25^{lo}Foxp3$^+$CD4$^+$ T cells into mice that we immunized with type II collagen 3 weeks before. One day after transfer, we subjected the mice to secondary immunization with collagen. We efficiently obtained Foxp3$^+$ cells by sorting hCD2$^+$ cells from *Foxp3*^{hCD2} knock-in mice[11]. hCD2-mediated enrichment of Foxp3$^+$ cells enabled us to isolate CD25^{lo}Foxp3$^+$ cells with high purity (**Supplementary Fig. 1**). We found that the transfer of CD25^{hi}Foxp3$^+$CD4$^+$, but not CD25^{lo}Foxp3$^+$CD4$^+$, T cells reduced joint swelling (**Fig. 1a**) and bone destruction (**Fig. 1b**) without affecting the production of collagen-specific antibodies (**Supplementary Fig. 2**). To examine the stability of Foxp3, we labeled donor CD25^{hi}Foxp3$^+$CD4$^+$ or CD25^{lo}Foxp3$^+$CD4$^+$ T cells with carboxyfluorescein succinimidyl ester (CFSE) and monitored Foxp3 expression in donor-derived (CFSE$^+$) CD4$^+$ T cells 1 week after secondary immunization. The majority of CD25^{hi}Foxp3$^+$CD4$^+$ T cells

[1]Department of Immunology, Graduate School of Medicine and Faculty of Medicine, The University of Tokyo, Bunkyo-ku, Tokyo, Japan. [2]Japan Science and Technology Agency (JST), Exploratory Research for Advanced Technology (ERATO) Program, Takayanagi Osteonetwork Project, Bunkyo-ku, Tokyo, Japan. [3]Department of Cell Signaling, Graduate School of Medical and Dental Sciences, Tokyo Medical and Dental University, Bunkyo-ku, Tokyo, Japan. [4]JST, Precursory Research for Embryonic Science and Technology Program, Bunkyo-ku, Tokyo, Japan. [5]Global Center of Excellence (GCOE) Program, International Research Center for Molecular Science in Tooth and Bone Diseases, Bunkyo-ku, Tokyo, Japan. [6]Laboratory for Systems Biology and Medicine, Research Center for Advanced Science and Technology, The University of Tokyo, Meguro-ku, Tokyo, Japan. [7]Department of Orthopaedic Surgery, Faculty of Medicine, The University of Tokyo, Tokyo, Japan. [8]Diabetes Center, University of California, San Francisco, San Francisco, California, USA. [9]Centre for Orthopaedic Research, School of Surgery, The University of Western Australia, Nedlands, Western Australia, Australia. Correspondence should be addressed to H.T. (takayana@m.u-tokyo.ac.jp).

Received 31 August; accepted 19 November; published online 22 December 2013; doi:10.1038/nm.3432

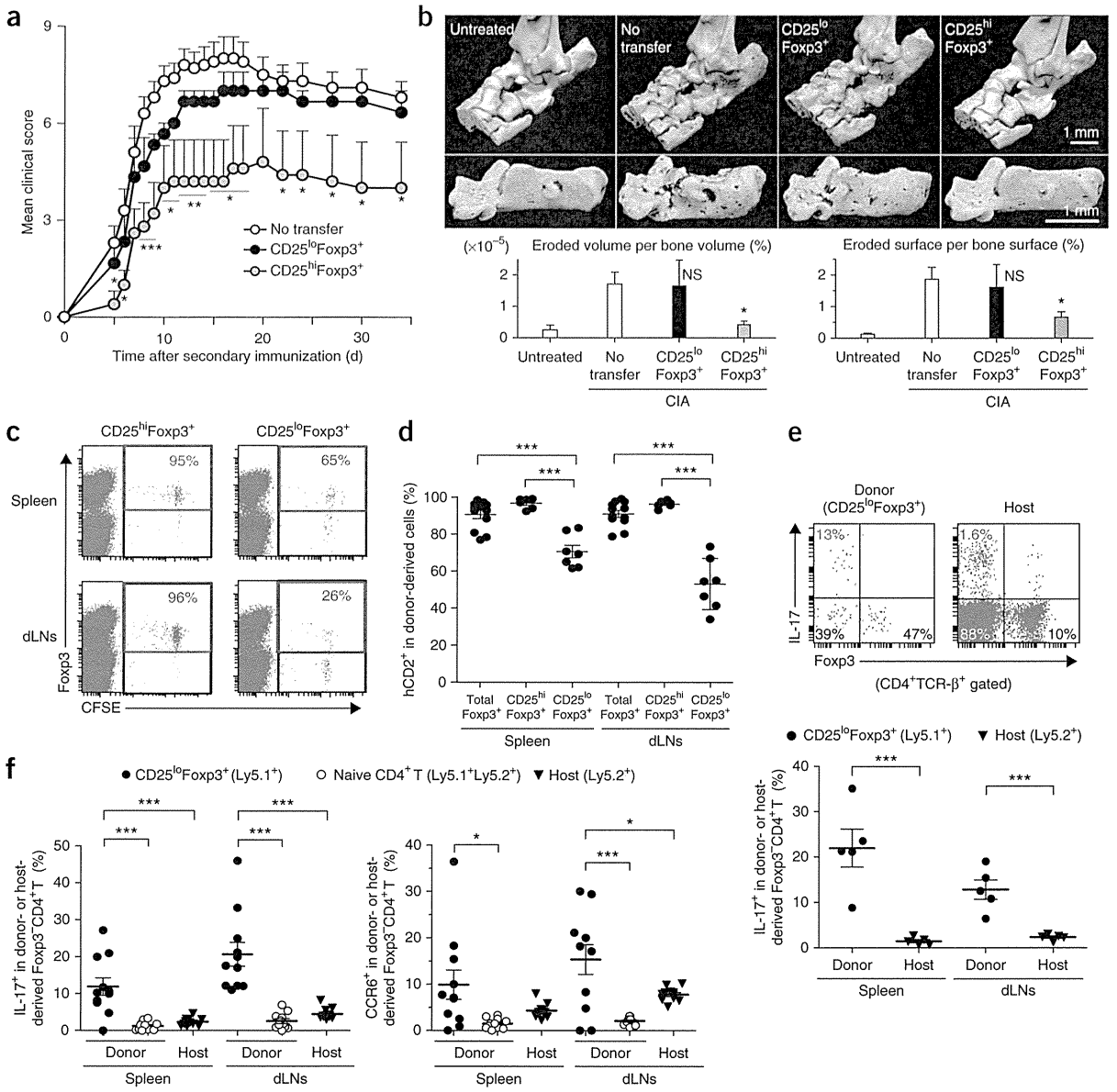

Figure 1 CD25^{lo}Foxp3^{+} T cells are unstable Foxp3^{+} T cells that convert to T_H17 cells under arthritic conditions. (**a**,**b**) Clinical score (**a**) and microcomputed tomography analysis of calcaneus in the ankle joints (**b**) of immunized DBA/1 mice adoptively transferred with 5×10^5 CD25^{hi} (**a**, $n = 3$; **b**, $n = 6$) or CD25^{lo} (**a**, $n = 5$; **b**, $n = 10$) Foxp3^{+}CD4^{+} T cells purified from untreated DBA/1 *Foxp3*^{hCD2} mice. (**c**) Frequency of Foxp3^{+} cells in CFSE^{+} donor-derived T cells. Representative data of five mice are shown. (**d**,**e**) Results from the immunized C57BL/6 Ly5.2 mice that were adoptively transferred with total hCD2^{+} ($n = 12$), CD25^{hi} ($n = 6$) or CD25^{lo} ($n = 7$) Foxp3^{+}CD4^{+} T cells from untreated B6.Ly5.1 *Foxp3*^{hCD2} mice. (**d**) Frequency of hCD2^{+} cells in donor-derived CD4^{+} T cells. (**e**) Top, representative plots of Foxp3 and IL-17 expression in CD25^{lo}Foxp3^{+} donor- or host-derived CD4^{+} T cells. Bottom, quantitative analysis of the frequency of IL-17^{+} cells in Foxp3^{-}CD4^{+} T cells derived from CD25^{lo}Foxp3^{+} donor or host cells ($n = 5$). (**f**) Frequency of IL-17^{+} (left) or CCR6^{+} (right) cells in Foxp3^{-}CD4^{+} T cells derived from CD25^{lo}Foxp3^{+} (Ly5.1^{+}Ly5.2^{-}) or naive CD4^{+} T (Ly5.1^{+}Ly5.2^{+}) donor cells or host cells (Ly5.1^{-}Ly5.2^{+}) ($n = 10$). All data are shown as the mean ± s.e.m. Statistical analyses were performed using unpaired two-tailed Student's *t* test (*$P < 0.05$, **$P < 0.01$, ***$P < 0.005$; NS, not significant). Each dot indicates a single mouse.

(>95%) retained Foxp3 expression, but CD25^{lo}Foxp3^{+}CD4^{+} T cells lost Foxp3 expression in the spleen (35%) and draining lymph nodes (dLNs) (75%) under arthritic conditions (**Fig. 1c**). These results suggest that the transferred CD25^{lo}Foxp3^{+}CD4^{+} T cells failed to inhibit inflammation and bone destruction because of their loss of Foxp3.

To follow the transferred cells for a longer period of time, we used donor T cells from B6 Ly5.1^{+} *Foxp3*^{hCD2} congenic mice and analyzed Foxp3 and IL-17 expression 2 weeks after secondary immunization in donor-derived Ly5.1^{+}CD4^{+} T cells in host mice with arthritis. The majority of transferred total Foxp3^{+} or CD25^{hi}Foxp3^{+} T cells retained Foxp3 expression, which is consistent with a previous report[10]. In contrast, when we purified and transferred CD25^{lo}Foxp3^{+}CD4^{+} T cells to the arthritic mice, these cells lost Foxp3 expression (30–50%) (**Fig. 1d**), and the percentage of IL-17–expressing cells in the donor-derived Foxp3^{-}CD4^{+} T cells (10–25%) was much greater than that in host-derived Foxp3^{-}CD4^{+} T cells (<3%) (**Fig. 1e** and **Supplementary Fig. 3**). Thus CD25^{lo}Foxp3^{+}CD4^{+} T cells preferentially lose Foxp3 and produce IL-17 in arthritic mice after adoptive transfer.

To determine the contribution of naive CD4^{+} and CD25^{lo}Foxp3^{+}CD4^{+} T cells to T_H17 cell development under arthritic

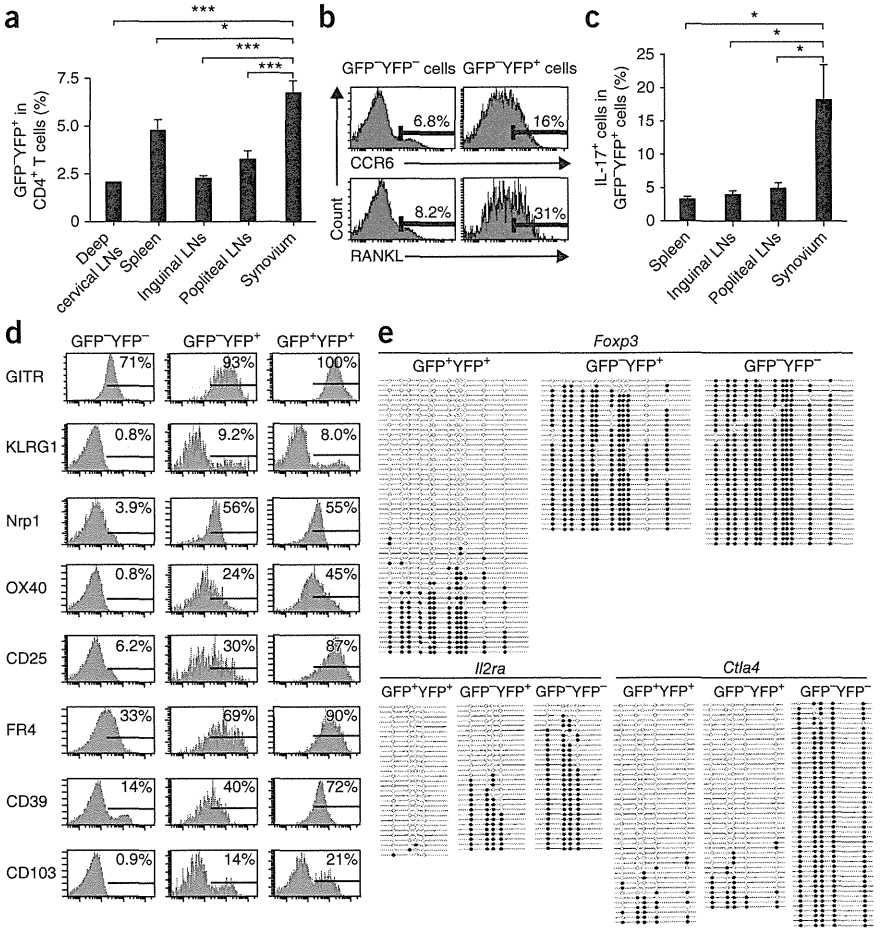

Figure 2 Localization, marker gene expression and DNA methylation status of exFoxp3 T cells in arthritic mice. Results are shown from fate mapping analyses of arthritic Foxp3-GFP-Cre × ROSA26-YFP mice that were performed 2 weeks after secondary immunization. (**a**) Frequency of exFoxp3 (GFP$^-$YFP$^+$) cells in CD4$^+$ T cells isolated from the indicated location ($n = 3$ for deep cervical LNs, $n = 8$ for all other groups). (**b**) Expression of CCR6 and RANKL in the indicated T cell populations in popliteal lymph nodes. Representative data of six independent experiments are shown. (**c**) Frequency of IL-17$^+$ cells in the GFP$^-$YFP$^+$ cell population ($n = 6$). (**d**) Expression of multiple T_{reg} cell phenotypic markers in exFoxp3 T cells. Representative data of six independent experiments are shown. The percentages in each plot show the frequency of positive cells (indicated by the horizontal lines). (**e**) CpG methylation of the *Foxp3*, *Il2ra* and *Ctla4* loci in exFoxp3 (GFP$^-$YFP$^+$), GFP$^+$YFP$^+$ and GFP$^-$YFP$^-$CD4$^+$ T cells. A horizontal row within each box corresponds to one sequenced clone in which specific CpGs were methylated (closed) or demethylated (open). All data are shown as the mean ± s.e.m. Statistical analyses were performed using unpaired two-tailed Student's *t* test (*$P < 0.05$, ***$P < 0.005$).

conditions, we transferred Ly5.1$^+$Ly5.2$^+$ naive CD4$^+$ and Ly5.1$^+$CD25^{lo}Foxp3$^+$CD4$^+$ T cells into immunized Ly5.2$^+$ mice, which we analyzed 2 weeks after secondary immunization. CD25^{lo}Foxp3$^+$ donor-derived Ly5.1$^+$Foxp3$^-$CD4$^+$ T cells expressed the T_H17 markers IL-17 and CCR6 (refs. 13,14) to a much greater extent than did naive CD4$^+$ donor-derived or host-derived Foxp3$^-$CD4$^+$ T cells (**Fig. 1f**). These findings suggest that under arthritic conditions, CD25^{lo}Foxp3$^+$CD4$^+$ T cells are prone to differentiate into T_H17 cells that are known to have a key pathological role in arthritis[13–18].

Characterization of exFoxp3 T cells in arthritic mice

To monitor the localization of exFoxp3 T cells *in vivo*, we crossed *Foxp3* bacterial artificial chromosome transgenic mice expressing the GFP-Cre recombinase fusion protein[7] with ROSA26-YFP reporter mice[19]. GFP indicates cells that are currently expressing Foxp3, whereas YFP marks cells that are expressing or did express Foxp3. Under arthritic conditions, the percentage of exFoxp3 (GFP$^-$YFP$^+$) cells (as a proportion of total CD4$^+$ T cells) was higher in joints than in other lymphoid organs (**Fig. 2a** and **Supplementary Fig. 4**), suggesting a preferential accumulation of exFoxp3 T cells in the synovium. In addition, exFoxp3 (GFP$^-$YFP$^+$) T cells expressed higher levels of CCR6 and RANKL than did GFP$^-$YFP$^-$ T cells in popliteal LNs (**Fig. 2b**). Notably, the percentage of IL-17$^+$ cells among exFoxp3 T cells was highest in arthritic joints (**Fig. 2c**). These results collectively indicate that *in vivo*, exFoxp3 T cells acquire an activated T_H17 phenotype (exFoxp3 T_H17 cells) and accumulate in the inflamed synovium.

Instability of Foxp3$^+$ T_{reg} cells under pathological conditions *in vivo* has been contentious, as the origin of this Foxp3-unstable population remains unclear. There are three possibilities for the origin of exFoxp3 T cells: thymus-derived T_{reg} (tT_{reg}) cells, peripherally derived T_{reg} (pT_{reg}) cells and activated conventional T cells that transiently express Foxp3 (refs. 20,21). T_{reg} cells are defined by their suppressive function and are characterized by the expression and demethylated status of Foxp3 and other T_{reg} cell signature genes[20,22]. Flow cytometric analysis indicated that GITR (also called TNFRSF18), neuropilin 1 (Nrp1) and killer cell lectin-like receptor subfamily G member 1 (KLRG1) were similarly expressed by exFoxp3 T cells and GFP$^+$YFP$^+$ T cells (**Fig. 2d**). exFoxp3 T cells also expressed CD25, folate receptor 4 (FR4), OX40 (also called TNFRSF4), CD39 (also called ENTPD1), CD103 (also called ITGAE) and cytotoxic T lymphocyte–associated protein 4 (CTLA-4), albeit to a lesser extent compared to GFP$^+$YFP$^+$ T cells (**Fig. 2d** and **Supplementary Fig. 5**). Thus, although the expression level of a few T_{reg} marker genes, including CD25 and FR4, was lower in exFoxp3 T cells than in GFP$^+$YFP$^+$ T cells, exFoxp3 T cells expressed most of the phenotypic T_{reg} markers and were distinguishable from activated conventional T cells that transiently express Foxp3 (**Fig. 2d**).

Methylation analysis of the *Foxp3*, *Il2ra* and *Ctla4* loci[22] in exFoxp3 T cells isolated from spleens and dLNs of arthritic mice revealed that the *Foxp3* locus was largely methylated and the *Il2ra* locus was partially methylated in exFoxp3 (GFP$^-$YFP$^+$) T cells (**Fig. 2e**). As the *Foxp3* locus in tT_{reg} cells is known to be demethylated[22], the data suggest that exFoxp3 T cells are not derived from tT_{reg} cells. The *Ctla4* locus of exFoxp3 T cells was demethylated, making these cells distinct from effector memory T cells and *in vitro*–induced T_{reg} cells[22].

Genome-wide expression analysis showed that exFoxp3 T_H17 cells highly express *Cxcr5*, *Ccr8*, *Rora* and *Rorc*, which are preferentially expressed in pT_{reg} cells that are generated through antigen delivery or in T_{reg} cells in the gut lamina propria[23] (**Supplementary Fig. 6**), but have lower expression of *Ikzf2* (encoding Helios) (**Supplementary Figs. 5** and **6**). These results suggest that exFoxp3 T_H17 cells may